

# B Lymphocyte Signaling Established by the CD19/CD22 Loop Regulates Autoimmunity in the Tight-Skin Mouse

Noriko Asano,<sup>\*†</sup> Manabu Fujimoto,<sup>\*</sup>  
Norihiro Yazawa,<sup>\*†</sup> Senji Shirasawa,<sup>‡</sup>  
Minoru Hasegawa,<sup>§</sup> Hitoshi Okochi,<sup>\*</sup>  
Kunihiko Tamaki,<sup>†</sup> Thomas F. Tedder,<sup>¶</sup> and  
Shinichi Sato<sup>§</sup>

From the Departments of Regenerative Medicine\* and Pathology,<sup>‡</sup> Research Institute, International Medical Center of Japan, Tokyo, Japan; the Department of Dermatology,<sup>†</sup> Faculty of Medicine, University of Tokyo, Tokyo, Japan; the Department of Dermatology,<sup>§</sup> Kanazawa University Graduate School of Medical Science, Ishikawa, Japan; and the Department of Immunology,<sup>¶</sup> Duke University Medical Center, Durham, North Carolina

**Systemic sclerosis (SSc) is characterized by fibrosis and autoimmunity. Peripheral blood B cells from SSc patients specifically overexpress CD19, a critical cell-surface signal transduction molecule in B cells. CD19 deficiency in B cells also attenuates skin fibrosis in the tight-skin (TSK/+) mouse, a genetic model for SSc. Herein we analyzed two transgenic mouse lines that overexpress CD19. Remarkably, 20% increase of CD19 expression in mice spontaneously induced SSc-specific anti-DNA topoisomerase I (topo I) antibody (Ab) production, which was further augmented by 200% overexpression. In TSK/+ mice overexpressing CD19, skin thickness did not increase, although anti-topo I Ab levels were significantly augmented, indicating that abnormal CD19 signaling influences autoimmunity in TSK/+ mice and also that anti-topo I Ab does not have a pathogenic role. The molecular mechanisms for abnormal CD19 signaling were further assessed. B-cell antigen receptor crosslinking induced exaggerated calcium responses and augmented activation of extracellular signal-regulated kinase in TSK/+ B cells. CD22 function was specifically impaired in TSK/+ B cells. Consistently, CD19, a major target of CD22-negative regulation, was hyperphosphorylated in TSK/+ B cells. These findings indicate that reduced inhibitory signal provided by CD22 results in abnormal activation of signaling pathways including CD19 in TSK/+ mice and also suggest that this disrupted B cell signaling contribute to specific autoantibody production. (*Am J Pathol* 2004, 165:641–650)**

Systemic sclerosis (SSc) is a multisystem disease characterized by fibrosis and autoimmunity.<sup>1</sup> SSc patients develop excessive extracellular matrix deposition in the skin and other visceral organs, resulting in fibrotic changes.<sup>2</sup> The tight-skin (TSK) mouse is a genetic animal model for SSc, which was originally identified as a spontaneous mutation that results in increased synthesis and excessive accumulation of collagen and other extracellular matrix proteins in the skin and visceral organs.<sup>3</sup> Although homozygous mice die *in utero*, heterozygous (TSK/+) mice survive, but develop cutaneous fibrosis resembling human SSc, if not identical.<sup>3,4</sup> TSK mutation is a tandem duplication within the gene encoding fibrillin 1, an extracellular matrix glycoprotein crucial for microfibril assembly.<sup>5</sup> TSK mutation causes a formation of the conformationally abnormal microfibrils, although it cannot account for all of the phenotypic abnormalities in TSK/+ mice.

The autoimmune aspect is another prominent feature of SSc.<sup>6</sup> Antinuclear antibodies (Abs) are found in the sera from >95% of SSc patients, and the associations between some specific antinuclear Abs and clinical manifestations are well established.<sup>7</sup> Autoantibody (autoAb) to DNA topoisomerase I (topo I) is detected most exclusively in SSc and correlated with diffuse cutaneous involvement, peripheral vascular disease, and pulmonary interstitial fibrosis.<sup>8</sup> TSK mice also have a skewed humoral response and produce anti-topo I Abs.<sup>9</sup> Although the relationship between fibrosis and systemic autoimmunity is unclear in TSK/+ mice, we recently demonstrated that B-cell functional defects caused by the loss of CD19, a B-cell-specific cell-surface molecule, significantly decreased skin fibrosis in TSK/+ mice, suggesting that B cells play an important role in the pathogenesis of these disorders of humans and mice.<sup>10</sup>

Recent studies using animal models of autoimmune diseases have revealed that B cells play various important roles, including antigen presentation and cytokine production as well as pathogenic autoAb production.

---

Supported by the Ministry of Education, Science, and Culture of Japan (grant-in-aid to M.F. and S.S.); the Mochida Memorial Foundations (to M.F.); and the National Institutes of Health (grants CA81776 and CA54464 to T.F.T.).

Accepted for publication April 9, 2004.

Address reprint requests to Manabu Fujimoto, M.D., Department of Dermatology, Faculty of Medicine, University of Tokyo, 7-3-1 Hongo, Bunkyo, Tokyo, 113-8655, Japan. E-mail: fujimoto-m@umin.ac.jp.

Elimination of B cells in the lupus-prone MRL/lpr mice results in a complete abrogation of nephritis, vasculitis, and skin disease, which is independent of Ab secretion.<sup>11</sup> Pathogenic autoAb production is also important as K/BxN mice, a model for rheumatoid arthritis, have hyperactive B cells that produce arthritogenic autoAb.<sup>12</sup> Consistently, recent studies have shown that B cell depletion by anti-CD20 Ab is effective in treating patients with rheumatoid arthritis or systemic lupus erythematosus.<sup>13–15</sup> Thus, B cells have recently attracted much attention as a crucial player in systemic autoimmune disorders.<sup>16</sup>

B cell fate and functions are primarily determined by signal transduction through a B-cell antigen receptor (BCR), which is further regulated by other cell-surface receptors that inform B cells of their extracellular micro-environment, including CD19, CD21, CD22, CD40, CD72, and Fc $\gamma$ RIIB. Among them, the CD19/CD21 complex serves as a positive regulator that amplifies BCR signal transduction for a prompt and strong immune response. When CD19/CD21 is cross-linked with C3d fragment of activated C3, this allows B cells to respond antigens with 10- to 1000-fold lower concentration.<sup>17</sup> By contrast, negative regulators such as CD22 are crucial for terminating BCR signal transduction and thus for avoiding improper immune response such as against self-antigens.<sup>18</sup>

We reported that circulating B cells from SSc patients overexpress CD19 by 20%. Strikingly, the current study revealed that this relatively small increase of CD19 expression in C57BL/6 mouse induced spontaneous production of SSc-specific anti-topo I autoAbs. Similarly, CD19 signaling was augmented in TSK/+ B cells that produced anti-topo I Abs. Therefore, we further assessed how B cell signaling was disturbed in TSK/+ mice. The present study showed that negative regulation provided by CD22 was disrupted in TSK/+ B cells, which resulted in abnormal activation of downstream signal transduction molecules including CD19. The results of this study may provide an important clue of how signaling pathways might be functionally disrupted in human patients with rheumatic diseases.

## Materials and Methods

### Mice

TSK/+ (the C57BL/6 background) mice were purchased from the Jackson Laboratory (Bar Harbor, ME). Human CD19-transgenic (TG)-1 mice (C57BL/6  $\times$  B6/SJL), CD19TG-4 mice (C57BL/6  $\times$  B6/SJL), and CD22-deficient (CD22<sup>-/-</sup>) mice (C57BL/6  $\times$  129) were described previously.<sup>19,20</sup> CD19TG-1, CD19TG-4, and CD22<sup>-/-</sup> mice were backcrossed more than four generations onto the C57BL/6 background before use in these studies. CD19TG-1 and CD19TG-4 TSK/+ mice were generated through breedings of CD19TG<sup>+/-</sup>TSK/+ mice. Cell-surface CD19 and CD22 expressions were verified by two-color fluorescence cytometry. To verify the TSK/+ genotype, polymerase chain reaction amplification of a

partially duplicated fibrillin 1 gene was performed using genomic DNA from each mouse as described.<sup>21</sup> Wild-type littermates generated from heterozygous matings were used appropriately as controls. All mice were housed in a specific pathogen-free barrier facility. Mice used in this study were 8 to 10 weeks of age. All studies and procedures were approved by the Animal Care Committee of International Medical Center of Japan and Kanazawa University School of Medicine.

### Reagents and Immunofluorescence Analysis

Monoclonal antibodies (mAbs) used included: anti-B220 (RA3-6B2; Beckman Coulter, Miami, FL); anti-CD19 (MB19.1<sup>22</sup>); anti-CD22 (MB22-1<sup>23</sup>, Cy34; BD PharMingen, San Jose, CA); anti-I-A (M5/114.15.2, BD PharMingen); and anti-phosphotyrosine Abs (4G10; Upstate Biotechnology, Lake Placid, NY; PY99, Santa Cruz Biotechnology, Santa Cruz, CA). Antisera used included: fluorescein isothiocyanate (FITC)-conjugated anti-IgM (Southern Biotechnology Associates, Inc., Birmingham, AL); F(ab')<sub>2</sub> fragments of goat anti-mouse IgM (Cappel, ICN Biomedicals, Irvine, CA); anti-Lyn, anti-Syk, anti-PLC $\gamma$ 2, anti-ERK2, and anti-JNK1 (Santa Cruz Biotechnology); anti-SHP-1 (Upstate Biotechnology); anti-Akt, anti-phospho-Akt (Ser473), and anti-phosphoCD19 (Y513) (Cell Signaling, Beverly, MA); anti-active ERK and anti-active JNK Abs (Promega, Madison, WI). Rabbit anti-phosphoCD22 (Y762) was generated by immunizing phosphotyrosine peptide of the sequence.

Immunofluorescence analysis was performed as described.<sup>22</sup> Briefly, leukocytes from blood and spleen were stained at 4°C using predetermined optimal concentrations of Abs for 20 minutes. Blood erythrocytes were lysed after staining using the Whole Blood Immuno-Lyse kit (Beckman Coulter). Cells with the forward and side light scatter properties of lymphocytes were analyzed on an Epics Altra flow cytometer (Beckman Coulter). Positive and negative populations of cells were determined using unreactive isotype-matched Abs (Beckman Coulter) as controls for background staining. To stain phosphotyrosine intracellularly, cells were fixed and permeabilized using Cytofix/Cytoperm kit (BD Biosciences, San Jose, CA).

### Enzyme-Linked Immunosorbent Assays (ELISAs) for AutoAbs

Serum anti-topo I autoAb levels were determined with specific ELISA kits (Medical and Biological Laboratories, Nagoya, Japan). Briefly, 96-well microtiter plates coated with topo I were incubated with serum samples diluted 1:100. The bound Abs were detected with alkaline phosphatase-conjugated anti-mouse IgG or IgM Abs (Southern Biotechnology Associates, Inc.). Relative levels of autoAbs were determined for each group of mice using pooled serum samples. Sera were diluted at log intervals (1:10 to 1:10<sup>5</sup>) and assessed for relative autoAb levels as above except the results were plotted as optical density versus dilution (log scale). The dilutions of sera giving

half-maximal optical density values were determined by linear regression analysis, thus generating arbitrary unit per milliliter values for comparison between sets of sera.

### *Assessment of Skin Fibrosis*

All skin sections were taken from the para-midline, lower back region (the same anatomical site to minimize regional variations in thickness) as full thickness sections extending down to the body wall musculature. Tissues were fixed in 10% formaldehyde solution for 24 hours and embedded in paraffin. Sections were stained with hematoxylin and eosin. Hypodermal thickness, which was defined as the thickness of a subcutaneous loose connective tissue layer (ie, the hypodermis or superficial fascia) beneath the panniculus carnosus, was measured for multiple transverse perpendicular sections using an ocular micrometer. The skin from male mice was generally thicker than that from female mice despite the presence or absence of TSK mutations (data not shown). Because similar results were obtained when male or female mice were analyzed separately, only data from female mice were presented for skin thickness and hydroxyproline content in this study.

### *B Cell Activation, Immunoprecipitations, and Western Blot Analysis*

Splenic B cells were purified by removing T cells with anti-Thy1.2 Ab-coated magnetic beads (DynaL, Inc., Lake Success, NY) and resuspended in RPMI 1640 medium containing 5% fetal calf serum. Cells were stimulated with F(ab')<sub>2</sub> fragments of goat anti-mouse IgM Ab (40 μg/ml) at 37°C. To examine antigen-specific B cells, mice were immunized by an intraperitoneal injection with 50 μg of 2,4,6-trinitrophenol (TNP)-conjugated ficoll (Biosearch Technologies, Novato, CA) in phosphate-buffered saline with complete Freund's adjuvant (Difco, Detroit, MI). Splenic B cells were harvested on day 7, stimulated with FITC-conjugated TNP-ficoll (Biosearch Technologies), and analyzed by flow cytometry. For sodium dodecyl sulfate-polyacrylamide gel electrophoresis (SDS-PAGE) or subjected to immunoprecipitation, cells were lysed in buffer containing 1% Nonidet P-40, 150 mmol/L NaCl, 50 mmol/L Tris-HCl (pH 8.0), 1 mmol/L Na orthovanadate, 2 mmol/L ethylenediaminetetraacetic acid, 50 mmol/L NaF, and protease inhibitors. For immunoprecipitations, cell lysates were precleared twice by incubation with control Abs plus protein G-Sepharose beads (Amersham Pharmacia Biotech, Buckinghamshire, UK), followed by incubation with protein G-beads plus Abs to proteins of interest for 4 hours at 4°C. For CD19 immunoprecipitations, lysates were precleared with Affigel 10 beads (Bio-Rad Laboratories, Hercules, CA) conjugated with mouse IgA, then incubated with Affigel 10 beads bearing anti-CD19 Ab (MB19.1). Immunoprecipitated proteins were subjected to SDS-PAGE, and transferred onto nitrocellulose membranes for immunoblotting. The membranes were incubated with peroxidase-conjugated Abs. The blots

were developed using an enhanced chemiluminescence kit (Pierce, Rockford, IL) and detected using Fluoro-S imager (Bio-Rad Laboratories). The blots were reprobbed with Abs specific for the protein of interest. Band intensity was quantified using Quantity One software (Bio-Rad Laboratories).

### *Measurement of [Ca<sup>2+</sup>]<sub>i</sub>*

Spleen cells (10<sup>7</sup>/ml) in RPMI 1640 medium containing 5% fetal calf serum and 10 mmol/L HEPES were loaded with 1 μmol/L indo-1-AM ester (Molecular Probes, Eugene, OR) at 37°C for 30 minutes. Cells were stained with FITC-conjugated anti-B220 for 15 minutes. The ratio of fluorescence (488/407 nm) of B220<sup>+</sup> cells was determined using an Epics Altra flow cytometer (Beckman Coulter). Baseline fluorescence ratios were collected for 1 minute before F(ab')<sub>2</sub> anti-mouse IgM Ab (10 or 40 μg/ml) were added. Results were plotted as the fluorescence ratio at 15-second intervals with the background subtracted. Increased fluorescence ratios indicate increases in [Ca<sup>2+</sup>]<sub>i</sub>.

### *Statistical Analysis*

All data are shown as mean values ± SEM. The Mann-Whitney *U*-test was used for determining the level of significance of differences between sample means and Bonferroni's test was used for multiple comparisons.

## **Results**

### *Augmented Production of Anti-Topo I Ab by CD19 Overexpression*

We reported that circulating B cells from SSc patients overexpress CD19 by 20%.<sup>23</sup> To assess whether CD19 overexpression can induce SSc-specific autoAb production, we examined anti-topo I Ab production in transgenic mice that overexpress human CD19 specifically on B cells. Remarkably, 20% increase of CD19 expression in mice (CD19TG-4<sup>+/-</sup>) spontaneously induced IgG anti-topo I Ab production (Figure 1A). Furthermore, transgenic mice that overexpress 200% of endogenous CD19 levels (CD19TG-1<sup>+/+</sup>) showed prominent increase of both IgG and IgM anti-topo I autoAb levels in the sera (106- and 41-fold, *P* < 0.01, respectively; Figure 1A). Considering that CD19TG-1<sup>+/+</sup> mice have approximately twofold higher Ig levels than wild-type mice, the autoAb levels were still significantly higher when serum Ig levels were normalized (data not shown). Thus, the anti-topo I Ab levels correlated with the CD19 expression levels in B cells, indicating that abnormal CD19 signaling pathway is closely associated with SSc-related autoimmunity including anti-topo I Ab production.

TSK/+ mice have circulating anti-topo I Ab, and the loss of CD19 expression significantly decreases the autoAb titers.<sup>10</sup> We examined whether CD19 overexpres-

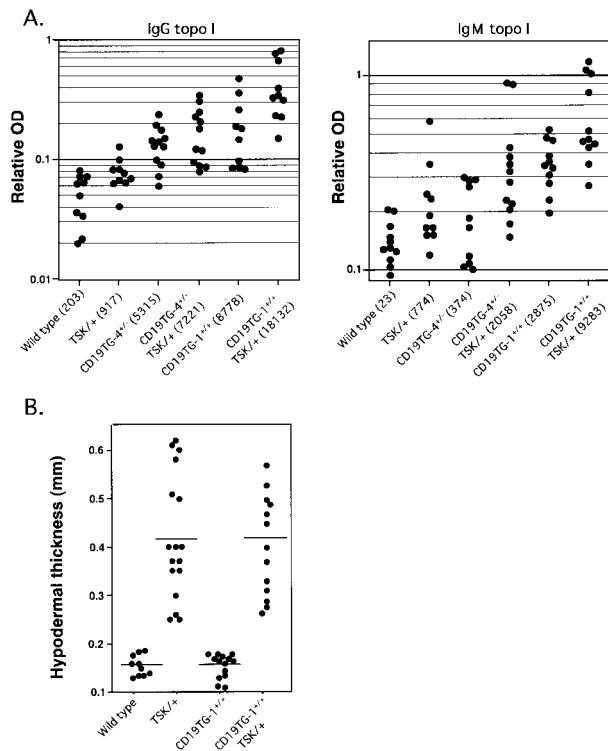


**Figure 1. A:** Serum levels of anti-topo I Abs in wild-type (WT), TSK/+, CD19TG-1<sup>+/+</sup>, CD19TG-4<sup>+/-</sup>, CD19TG-1<sup>+/+</sup>TSK/+, CD19TG-4<sup>+/-</sup>TSK/+ mice. Relative Ab levels were determined by Ig subclass-specific ELISA, with results from each mouse represented as a dot. Values in parentheses represent the dilutions of pooled sera giving half maximal optical density values in ELISA, which were determined by linear regression analysis to generate arbitrary units per milliliter that could be directly compared between each group of mice. **B:** Skin fibrosis in wild-type, CD19TG-1<sup>+/+</sup>, TSK/+, and CD19TG-1<sup>+/+</sup>TSK/+ mice. Skin tissues were taken from the dorsal site of mice. Hypodermal thickness was measured under a light microscope as the thickness from the top of granular layer to the bottom of a subcutaneous loose connective tissue layer (ie, the hypodermis or superficial fascia) beneath panniculus carnosus. Results from each mouse are represented as a single dot. Horizontal bars represent mean hypodermal thickness.

sion further increased the autoAb levels in TSK/+ mice. Both IgG and IgM anti-topo I Ab levels significantly increased in both lines of CD19TG/TSK/+ mice compared with TSK/+ mice (Figure 1A). Furthermore, augmentation of anti-topo I levels paralleled with the CD19 density on B cell surface of these transgenic mice (Figure 1A). IgG anti-topo I levels were 7.9-fold higher ( $P < 0.01$ ) in CD19TG-4<sup>+/-</sup>TSK/+ mice and 20-fold higher ( $P < 0.01$ ) in CD19TG-1<sup>+/+</sup>TSK/+ mice compared with TSK/+ mice (Figure 1A). Similarly, IgM anti-topo I levels in CD19TG-4<sup>+/-</sup>TSK/+ mice and CD19TG-1<sup>+/+</sup>TSK/+ mice were 2.7-fold ( $P < 0.05$ ) and 12-fold higher ( $P < 0.01$ ) than those in TSK/+ mice, respectively (Figure 1A). Therefore, CD19 overexpression enhanced anti-topo I Ab production in TSK/+ mice as well as C57BL/6 mice. Moreover, TSK genetic background in CD19TG-1<sup>+/+</sup> and CD19TG-4<sup>+/-</sup> mice resulted in significantly augmented anti-topo I Ab production relative to CD19TG-1<sup>+/+</sup> and CD19TG-4<sup>+/-</sup> mice, respectively (Figure 1A). Therefore, CD19 overexpression and TSK genetic background cooperatively contributed to anti-topo I Ab production.

### CD19 Overexpression Did Not Increase Skin Thickness

We previously reported that CD19 deficiency attenuates skin fibrosis in TSK/+ mice,<sup>10</sup> raising a possibility that CD19 may play a direct role in the induction of fibrosis. Therefore, we examined skin thickness in CD19TG mice. However, histopathology of the full-thickness skin sections from CD19TG-1<sup>+/+</sup> and CD19TG-4<sup>+/-</sup> mice showed normal hypodermal thickness compared with wild-type littermates (Figure 1B and data not shown). Skin content of hydroxyproline that is a modified amino acid uniquely found as a high percentage of collagen also showed no difference between CD19TG mice and wild-type littermates (data not shown). We then crossed CD19TG-1 and CD19TG-4 mice with TSK/+ mice to generate two TSK mouse lines that overexpress CD19 at different levels on B cells. However, hypodermal thickness and skin hydroxyproline content of TSK/+ mice were not altered by either level of CD19 overexpression (Figure 1B and data not shown). Collectively, although CD19 loss can decrease skin fibrosis of TSK/+ mice, CD19 overexpression did not increase skin fibrosis.

### Hyperreactive B-Cell Phenotype in TSK/+ Mice

Given that CD19 is a critical molecule that regulates B cell signaling, the finding that TSK/+ B cells exhibited the augmented anti-topo I Ab production that was enhanced by CD19 overexpression suggests that there are intrinsic signaling abnormalities of B cells in TSK/+ mice. Consistent with this, circulating B cells from TSK/+ mice expressed significantly lower levels of surface IgM ( $50 \pm 3\%$  decrease from wild-type mice,  $P < 0.05$ ; Figure 2A), zrf10 and higher levels of MHC class II (I-A) ( $30 \pm 7\%$  increase from wild-type mice,  $P < 0.05$ ; Figure 2B) than those from wild-type littermates. By contrast, there was no significant difference in splenic B cells with the expression levels of IgM or I-A between TSK/+ and wild-type littermates. The phenotypes observed in circulating B cells from TSK/+ mice was equivalent to B cells that demonstrate augmented transmembrane signaling through the BCR complex, such as CD22<sup>-/-</sup> mice and mice overexpressing CD19.<sup>24</sup> These mice also exhibit phenotypical abnormalities in circulating B cells, although the differences are usually mild in splenic B cells.<sup>22,25,26</sup> These changes appeared distinct because TSK/+ B cells expressed other cell surface molecules, including CD19, CD21, CD22, CD40, and B220 at similar levels as those from wild-type littermates (data not shown). Therefore, TSK/+ B cells exhibited distinctive hyperreactive phenotype.

### Augmented $[Ca^{2+}]_i$ Responses in TSK/+ B Cells

Because B cell phenotype from TSK/+ mice suggested that TSK/+ B cells were hyperresponsive to transmembrane signals, an increase in the intracellular calcium concentration ( $[Ca^{2+}]_i$ ) after BCR ligation was examined

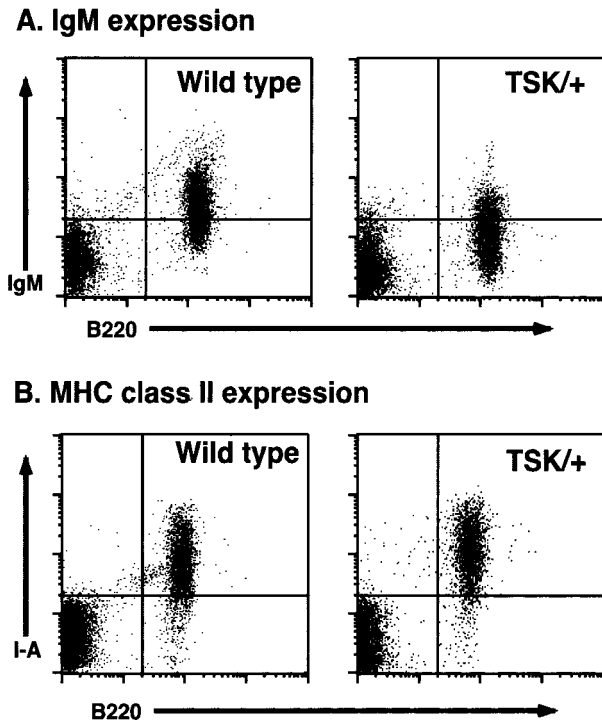


**Figure 2.** Cell surface expression of IgM (A) and MHC class II (I-A) (B) by blood mononuclear cells from TSK/+ mice or wild-type littermates. Single cell suspensions of leukocytes were isolated from wild-type and TSK/+ mice and examined by two-color immunofluorescence staining with flow cytometry analysis. These results are representative of those obtained in four similar experiments.

as an indicator of rapid B cell activation. Splenic B cells were freshly isolated from TSK/+ and wild-type littermates and were stimulated with F(ab')<sub>2</sub> fragments of anti-IgM Ab. TSK/+ B cells demonstrated significantly augmented rapid increase of [Ca<sup>2+</sup>]<sub>i</sub> as well as augmented sustained increase after IgM cross-linking when compared with wild-type B cells (Figure 3). In five experiments, maximum [Ca<sup>2+</sup>]<sub>i</sub> in TSK/+ B cells was 50% higher than wild-type B cells (*P* < 0.01). The kinetics of [Ca<sup>2+</sup>]<sub>i</sub> change was also slightly accelerated in TSK/+ B cells when compared with wild-type B cells. The augmented response in TSK/+ B cells did not result from a few exceptional B cells but represented most of B cells because the ratio of responding B cells from TSK/+ mice was equal to that of wild-type littermates (data not shown). Thus, BCR-induced [Ca<sup>2+</sup>]<sub>i</sub> response was augmented in TSK/+ B cells.

### Normal Phosphorylation Levels of Lyn, Syk, SHIP, PLCγ2, and Shc in TSK/+ B Cells

Because TSK/+ B cells were likely to be hyperresponsive to BCR cross-linking, tyrosine phosphorylation of B-cell signaling molecules was assessed to determine which pathways were responsible for this alteration. Lyn and Syk are protein tyrosine kinases abundantly expressed in B cells and have crucial roles in [Ca<sup>2+</sup>]<sub>i</sub> responses.<sup>27</sup> To assess Lyn and Syk phosphorylation, freshly isolated splenic B cells were stimulated with F(ab')<sub>2</sub> fragments of

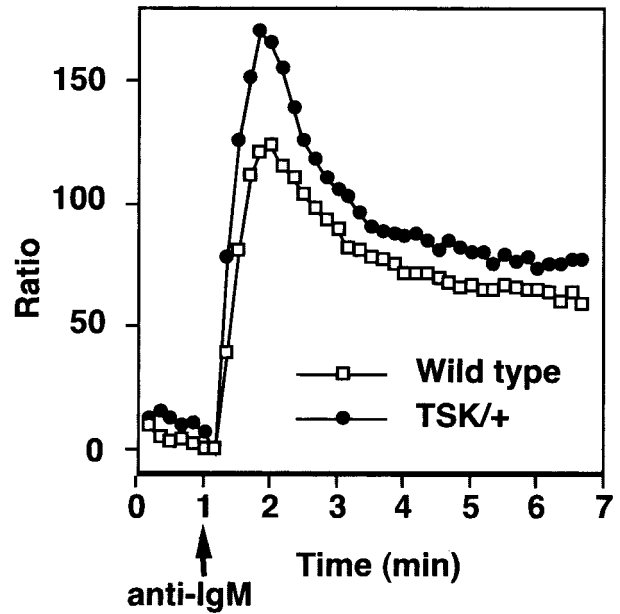


**Figure 3.** [Ca<sup>2+</sup>]<sub>i</sub> responses induced by BCR ligation. Spleen cells from wild-type or TSK/+ mice were loaded with 1 μmol/L indo-1-AM ester and then stained with FITC-conjugated anti-B220 to identify B cells. At 1 minute (arrow), goat anti-IgM F(ab')<sub>2</sub> fragments (40 μg/ml) were added. Results were plotted as the fluorescence ratio at 15-second intervals with the background subtracted. Increased ratios of indo-1 fluorescence indicate increased [Ca<sup>2+</sup>]<sub>i</sub>. Results represent three experiments.

anti-IgM Ab and were lysed at different time points after BCR cross-linking. Lyn or Syk was immunoprecipitated from lysates, followed by SDS-PAGE and anti-phosphotyrosine immunoblotting. Anti-IgM ligation induced Lyn phosphorylation at similar levels between wild-type and TSK/+ B cells (Figure 4A). Also, Syk was comparably phosphorylated in TSK/+ B cells on BCR engagement (Figure 4B). Therefore, tyrosine phosphorylation of these protein tyrosine kinases was intact in TSK/+ B cells. Also,

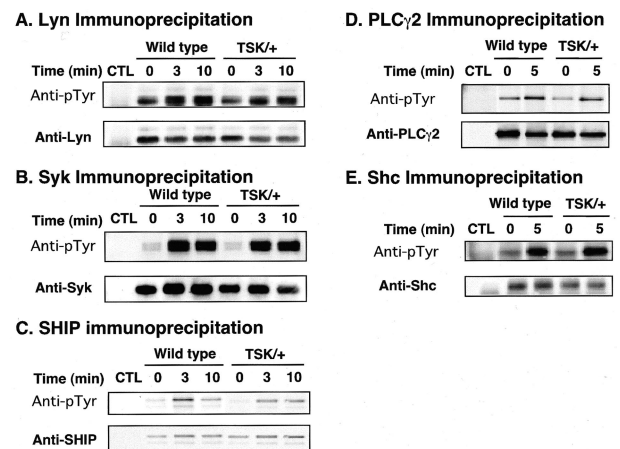


**Figure 4.** Phosphorylation of Lyn (A), Syk (B), PLCγ2 (C), SHIP (D), and Shc (E) after BCR ligation. Splenic B cells purified from TSK/+ or wild-type control littermates (1 × 10<sup>7</sup>/lane) were incubated with either medium alone (time 0) or with anti-IgM Ab (40 μg/ml) for the indicated times and lysed. Lysates were incubated with protein-G beads and either specific Ab or control rabbit IgG (CTL). Immunoprecipitated proteins were subjected to SDS-PAGE and transferred onto membranes for anti-pTyr immunoblotting. The blots were subsequently stripped and reprobed with appropriate Abs to verify equivalent loading of proteins between samples.

tyrosine kinase activities of Lyn and Syk determined by *in vitro* kinase assays were comparable between wild-type and TSK/+ B cells (data not shown).

Signaling mediators were then assessed for tyrosine phosphorylation. SHIP and PLC $\gamma$ 2 also regulate  $[Ca^{2+}]_i$  response negatively and positively, respectively.<sup>27</sup> However, despite the augmented  $[Ca^{2+}]_i$  response in TSK/+ B cells, SHIP phosphorylation was similar or slightly decreased in TSK/+ B cells (Figure 4C). BCR-induced phosphorylation of PLC $\gamma$ 2 was also similar or slightly had decreased levels in TSK/+ B cells (Figure 4D). Additionally, Shc was phosphorylated at wild-type level in TSK/+ B cells after BCR ligation (Figure 4E). Furthermore, phosphorylation level at tyrosine-317 of Shc was also similar between wild-type and TSK/+ B cells (data not shown). Therefore, these mediators were not responsible for augmented  $[Ca^{2+}]_i$  response in TSK/+ B cells.

### Modest CD22 Phosphorylation in TSK/+ B Cells

Because B cells from CD22<sup>-/-</sup> mice exhibit exaggerated  $[Ca^{2+}]_i$  response after BCR ligation,<sup>20,28-30</sup> CD22 would be another candidate for augmented  $[Ca^{2+}]_i$  mobilization in TSK/+ B cells. Therefore, CD22 phosphorylation was examined in TSK/+ B cells. Remarkably, constitutive tyrosine phosphorylation of CD22 in TSK/+ B cells was significantly lower than in wild-type B cells (47  $\pm$  35% of wild-type, Figure 5A). Furthermore, anti-IgM engagement induced only modest tyrosine phosphorylation of CD22 compared with wild-type B cells (58% of wild type at 5 minutes,  $P < 0.05$ ; Figure 5A). Consistent with this, SHP-1 association with CD22 was also decreased in TSK/+ B cells before and after BCR crosslinking (Figure 5A). These results raised the question whether CD22 function was defected in B cells from TSK/+ mice. Because CD19 is a major target of the CD22/SHP-1 inhibitory pathway,<sup>22</sup> CD19 tyrosine phosphorylation was further assessed in TSK/+ B cells. Consistent with decreased CD22 phosphorylation, CD19 was hyperphosphorylated after BCR ligation in TSK/+ B cells relative to wild-type B cells (Figure 5B). Overall, phosphorylation of CD19/CD22 loop was specifically dysregulated in TSK/+ B cells, which may lead to augmented  $[Ca^{2+}]_i$  responses.

To further confirm that the CD19/CD22 loop was dysregulated in TSK/+ B cells, antigen-specific B cells from TSK mice immunized with TNP-ficoll were assessed. After immunizing wild-type and TSK/+ mice with TNP-ficoll, splenic B cells were purified and stimulated with FITC-conjugated TNP-ficoll. Then, antigen-specific FITC-positive cells were analyzed for CD19 and CD22 tyrosine phosphorylation by flow cytometry. Similar to anti-IgM stimulation, CD19 phosphorylation was augmented by TNP stimulation in TSK/+ B cells compared with wild-type B cells (Figure 5C), while CD22 phosphorylation was also decreased by TNP stimulation in TSK/+ B cells (Figure 5C). Thus, the CD19/CD22 loop was dysregulated in antigen-specific B cells from TSK/+ mice.

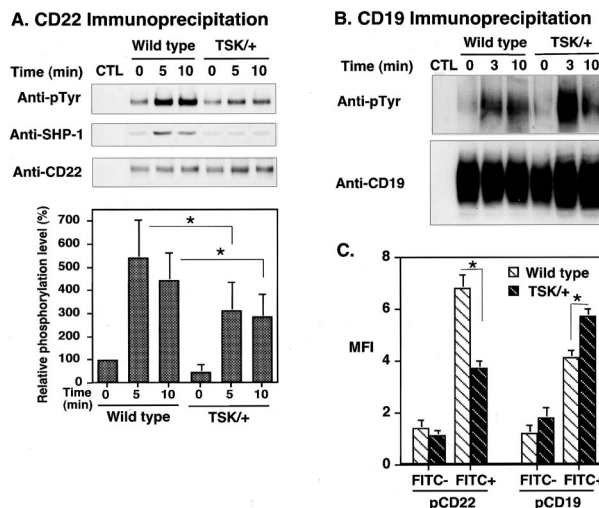


**Figure 5.** Phosphorylation of CD22 and CD19 after BCR ligation. **A** and **B:** Lysates of TSK/+ and wild-type B cells ( $10^7$ /lane) treated as in Figure 4, and CD22 or CD19 was immunoprecipitated from the lysate. Immunoprecipitated proteins were subjected to SDS-PAGE and transferred onto membranes for anti-pTyr and/or SHP-1 immunoblotting. The blots were subsequently stripped and reprobed with anti-CD22 or anti-CD19 Ab. Relative phosphorylation levels of CD22 are shown in the **bottom** graph which represent the relative mean optical density ( $\pm$  SEM) of band intensities determined by scanning densitometry from five independent immunoblotting experiments. Phosphorylation levels are shown as percentage of wild-type B cells at 0 minutes defined as 100%. **C:** Wild-type and TSK/+ mice were immunized with TNP-ficoll, and splenic B cells were purified on day 7. B cells were stimulated with FITC-conjugated TNP-ficoll for 5 minutes. FITC-positive (antigen-specific) and FITC-negative (not antigen-specific) cells were analyzed for CD19 and CD22 tyrosine phosphorylation by flow cytometry using anti-phosphoCD22 and anti-phosphoCD19 antibodies. FITC-negative cells showed no significant difference in CD22 and CD19 phosphorylation levels before and after stimulation. \*,  $<0.05$ .

### Activation of Downstream Signaling Pathways in TSK/+ B Cells

The consequence of impaired CD22 function was further studied in downstream signaling pathways such as mitogen-activated protein kinases (MAPKs) and Akt. Subfamilies of MAPKs include ERK, c-Jun N-terminal kinase (JNK), and p38, which become fully activated as a result of dual phosphorylation on single threonine and tyrosine residues. Activation of ERK, JNK, p38, and Akt after BCR stimulation was evaluated by immunoblotting using Abs specific for the fully active forms of ERK, JNK, p38, and Akt. Among MAPKs and Akt, only ERK activation exhibited enhanced phosphorylation by 65% in TSK/+ B cells when compared with wild-type B cells ( $P < 0.01$ , Figure 6A). Although JNK activation is dependent on  $[Ca^{2+}]_i$  response and TSK/+ B cells demonstrated elevated  $[Ca^{2+}]_i$  response, JNK activation in TSK/+ B cells reached at similar peak level but attenuated more rapidly than that of wild-type B cells (Figure 6B). Contrast to the previous studies, we could not detect significant phosphorylation of p38 after BCR cross-linking either in wild-type or TSK/+ B cells despite using several Abs (data not shown). Furthermore, Akt phosphorylation in TSK/+ B cells was at similar levels to that of wild-type B cells (Figure 6C). Thus, ERK activation was specifically increased in TSK/+ B cells.

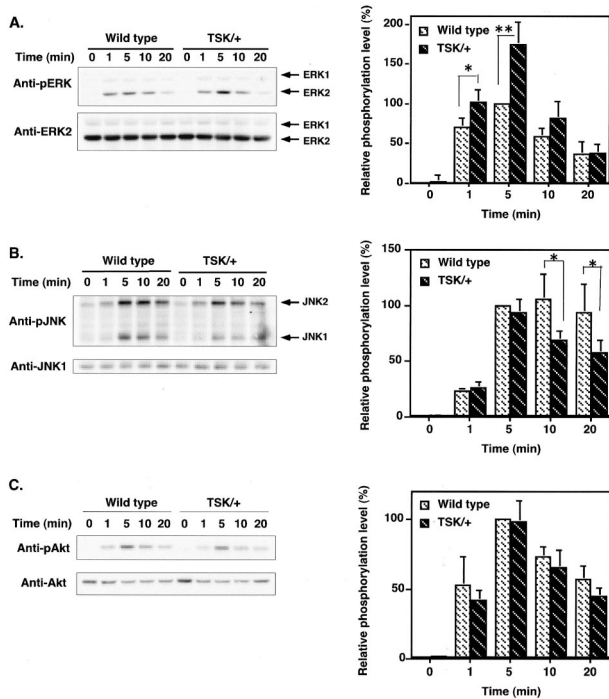


**Figure 6.** ERK (A), JNK (B), and Akt (C) activation induced by BCR ligation in TSK/+ B cells. Splenic B cells purified from TSK/+ or wild-type control littermates ( $1 \times 10^6$ /lane) were stimulated with anti-IgM. Subsequently, lysates of B cells were subjected to SDS-PAGE and transferred to nitrocellulose membranes for subsequent immunoblotting with phospho-specific Abs for the activated forms of the MAPKs and Akt. Results (left) are representative of those obtained with three littermate pairs of mice. Membranes were reprobed with anti-ERK2, anti-JNK1, and anti-Akt Abs. Values in the right graphs represent the relative mean optical density ( $\pm$ SEM) of band intensities determined by scanning densitometry from three independent immunoblotting experiments. Phosphorylation levels are shown as percentage of wild-type B cells at 0 minutes and 5 minutes were defined as 0% and 100%, respectively. \*,  $<0.05$ ; \*\*,  $<0.01$ .

### Hyperactivation of B Cells in TSK/+ Mice Was Dependent on CD22 Expression

To determine whether disruption of CD22 function was the dominant feature of TSK/+ B cells, TSK/+ mice deficient in CD22 expression (CD22<sup>-/-</sup>TSK/+ mice) were generated and compared with CD22<sup>-/-</sup> mice without TSK mutation. If CD22 function was specifically disrupted in TSK/+ B cells, the abnormalities of signal transduction would not be observed in the absence of CD22 expression and thus CD22<sup>-/-</sup>TSK/+ B cells would demonstrate similar signaling property to CD22<sup>-/-</sup> B cells without TSK mutation. Alternatively, if ERK activation observed in TSK/+ B cells was not related to CD22 dysfunction, CD22<sup>-/-</sup>TSK/+ B cells would exhibit more profound alteration than CD22<sup>-/-</sup> B cells or TSK/+ B cells. Remarkably, the [Ca<sup>2+</sup>]<sub>i</sub> responses in CD22<sup>-/-</sup>TSK/+ B cells were identical to those responses in B cells from CD22<sup>-/-</sup> mice after the optimal or suboptimal concentration of anti-IgM incubation (Figure 7A and data not shown). Furthermore, increased ERK phosphorylation was no longer observed in TSK/+CD22<sup>-/-</sup> B cells in response to BCR engagement when compared with CD22<sup>-/-</sup> B cells (Figure 7B). However, hypodermal thickness of TSK/+ mice was not altered by CD22 deficiency

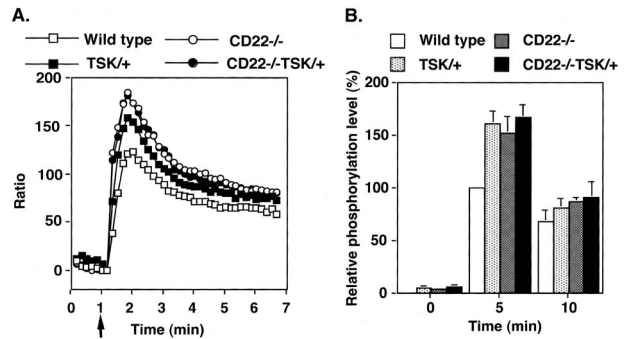


**Figure 7.** [Ca<sup>2+</sup>]<sub>i</sub> responses (A) and ERK activation (B) after BCR ligation in wild-type and CD22<sup>-/-</sup> B cells with or without TSK mutation. **A:** B cells loaded with indo-1 and stained with FITC-labeled anti-B220 were examined for relative [Ca<sup>2+</sup>]<sub>i</sub> levels by flow cytometry after gating on the B220<sup>+</sup> population of cells as described in Figure 3. Suboptimal concentration of goat anti-IgM F(ab')<sub>2</sub> fragments (10  $\mu$ g/ml) were added at 1 minute (arrow). **B:** BCR-induced ERK phosphorylation was assessed as in Figure 6.

(data not shown). Thus, hyperactivated signal transduction of B cells in TSK/+ mice was dependent on CD22 expression.

### Discussion

In the current study, roles of CD19 and B cell signaling in autoimmunity and disease expression of SSc were explored. SSc-specific anti-topo I Ab production was induced by 20%- increased CD19 expression, regardless of the presence of TSK mutation (Figure 1). By contrast, anti-fibrillin 1 Ab levels were not significantly increased in either strain of CD19TG mice compared with wild-type mice (data not shown). Although diminished B cell function by CD19 loss in TSK/+ mice improve skin fibrosis,<sup>10</sup> CD19 overexpression did not accelerate skin fibrosis in TSK/+ mice (Figure 1). Anti-topo I Ab levels are shown to correlate with severity of skin involvement and global disease severity of human SSc.<sup>31,32</sup> However, results of

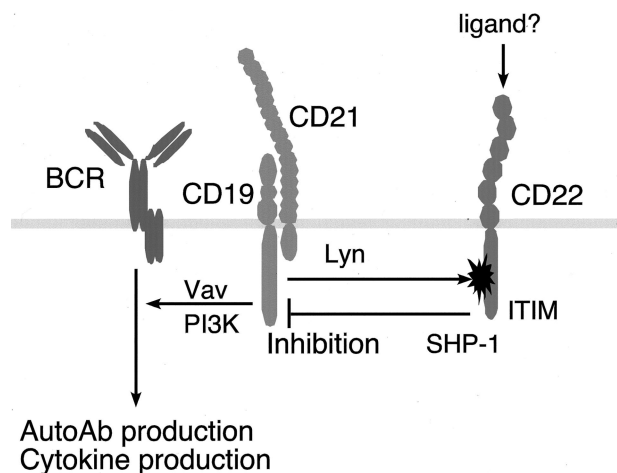


**Figure 8.** A proposed model for disrupted CD19/CD22 loop in TSK/+ B cells. CD22 phosphorylation by Lyn is specifically impaired possibly by the interaction with CD22 ligand(s). Alternatively, CD19 overphosphorylation may also affect CD22 phosphorylation. Decreased CD22 phosphorylation results in modest SHP-1 activation, which leads to hyperphosphorylation of CD19. This may up-regulate signaling pathways for autoAb production and cytokine production.

the present study suggest that anti-topo I Ab does not have direct pathogenic role in the fibrosis of SSc but is rather an epiphenomenon. Consistently, although anti-topo I Ab is highly useful as a diagnostic marker, topo I is an intracellular component critical for cell mitosis and there has been no evidence to show anti-topo I Ab is internalized into the cell. Nonetheless, anti-topo I Ab production in CD19TG mice is remarkable because most of other autoimmune strains of mice, including MRL/lpr and NZB/NZW mice, do not develop anti-topo I Ab. The only exception known to date is motheaten viable mice, which have defective SHP-1 function.<sup>33</sup> The current study also demonstrates that CD22 function was specifically impaired in TSK/+ B cells (Figure 5). CD22 has immunoreceptor tyrosine-based inhibitory motifs that recruit SHP-1 when phosphorylated. CD22 serves as an inhibitory signaling molecule and a major target of CD22/SHP-1 inhibitory pathway is CD19.<sup>22,33</sup> Consistently, CD19 phosphorylation was significantly augmented in both resting and BCR-ligated TSK/+ B cells (Figure 5B). As in TSK/+ B cells, B cells from motheaten viable mice also show CD19 hyperphosphorylation.<sup>33</sup> Collectively, these results indicate that negative regulation by CD22 was disrupted in TSK/+ B cells, which resulted in abnormal activation of downstream signal transduction molecules including CD19 (Figure 8), and also suggest that CD19/CD22 signaling pathways are closely associated with SSc-specific anti-topo I Ab production. Also, the discrepancy between anti-topo I Ab and skin fibrosis provides direct evidence that anti-topo I Ab does not have a pathogenic role.

Considering that there are no known genetic abnormalities in lymphocytes of TSK/+ mice, it was surprising that TSK/+ B cells have intrinsic abnormalities in BCR signal transduction, such as exaggerated  $[Ca^{2+}]_i$  responses (Figure 3) and augmented ERK activation (Figure 6A). Circulating B cells from TSK/+ mice exhibited characteristic phenotype of chronically activated B cells with constitutively lower surface IgM expression and constitutively elevated MHC class II and CD23 expression (Figure 2).<sup>19</sup> This phenotype is also shared by CD19TG mice, *Lyn*<sup>-/-</sup> mice, CD22<sup>-/-</sup> mice, and motheaten viable mice, and is considered as a consequence of augmented transmembrane signaling through the BCR complex.<sup>34</sup> Because CD19TG mice, *Lyn*<sup>-/-</sup> mice, CD22<sup>-/-</sup> mice, and motheaten viable mice all exhibit autoimmunity characterized by various spontaneous autoAb production, CD22 dysfunction in TSK/+ B cells may lead to autoAb production in TSK/+ mice by abrogating negative regulation on BCR signaling.

Although CD22 phosphorylation was markedly lower than wild-type B cells (Figure 5A), major tyrosine kinases in B cells, *Lyn* and *Syk*, showed normal expression and normal phosphorylation constitutively and on BCR ligation in TSK/+ B cells (Figure 4, A and B). Also, *Shc* and *PLC $\gamma$ 2* phosphorylation was of wild-type levels or slightly decreased in TSK/+ B cells (Figure 4, D and E). Therefore, CD22 dysfunction is not likely a consequence of disturbed upstream events or general signaling defect. CD22 is a major regulator of  $[Ca^{2+}]_i$  mobilization among a number of signaling molecules because B cells lacking CD22 display dramatically augmented  $[Ca^{2+}]_i$  responses

after BCR ligation.<sup>20,28-30</sup> Therefore, enhanced BCR-induced  $[Ca^{2+}]_i$  increase in TSK/+ B cells (Figure 3) was consistent with decreased levels of CD22 phosphorylation (Figure 5A). Furthermore, ERK phosphorylation in TSK/+ B cells was augmented by 60% when compared with wild-type B cells (Figure 6A). Because the absence of CD22 results in increased phosphorylation of ERK after BCR cross-linking,<sup>35</sup> the augmented ERK activation observed in TSK/+ B cells may be linked to dysregulated CD22 function as well. Consistently, ERK activation after BCR engagement was similar between CD22<sup>-/-</sup> TSK/+ B cells and CD22<sup>-/-</sup> B cells (Figure 7). By contrast to enhanced ERK phosphorylation, BCR-induced JNK phosphorylation was decreased in TSK/+ B cells (Figure 6B). This decreased JNK activation in TSK/+ mice might be intriguing because *c-jun* plays a regulatory role on the expression of collagen promoter. Although the mechanism is unclear, JNK activation is also impaired in B cells from CD22<sup>-/-</sup> mice.<sup>36</sup> This pattern of augmented ERK activity and decreased JNK activity was also observed in B cells from CD19TG mice (M.F. and T.F.T., unpublished observation). Therefore, B cells from TSK/+ mice, CD19TG mice, and CD22<sup>-/-</sup> mice share the hyperfunction (ie, hyperphosphorylation or overexpression) of CD19 and the hypofunction (ie, hypophosphorylation or deficiency) of CD22,<sup>37</sup> and thus this may be a common trait in autoimmune strains.

In resting B cells, CD22 is bound to endogenous sialic acid-containing ligands such as CD45 and IgM and is unavailable for binding to exogenous molecules.<sup>38</sup> This *cis*-binding may locate CD22 proximal to BCR or CD45, which may be necessary for inhibitory function of CD22.<sup>39,40</sup> This masking of CD22 by *cis*-binding can be relieved by the stimulation of anti-IgM and anti-CD40 Ab.<sup>38</sup> Because TSK/+ B cells have a chronically activated phenotype, CD22 on TSK/+ B cells may be unmasked and is available to *trans*-binding with unknown exogenous ligands that sequester CD22 from BCR. Indeed, preincubation of human B cells with anti-CD22 mAb has been shown to lower the threshold for BCR-induced proliferation and increase in  $[Ca^{2+}]_i$  signaling through the BCR.<sup>41</sup> Intriguingly, CD72, another negative regulator that has analogous functions to CD22, is demonstrated to undergo a unique regulation that soluble form of CD100 binds with CD72 and switches off the negative signals mediated by CD72.<sup>42</sup> Soluble CD100 protein released from activated lymphocytes is abnormally detected in the sera of the MRL/lpr mouse, an autoimmune strain with a defect in *Fas*.<sup>43</sup> Similarly, the ligand-binding site of CD22 appears to have a critical role in autoimmunity. In the mouse, CD22 is defined by *Lyb-8* alloantigen system, *Cd22<sup>a</sup>*, *Cd22<sup>b</sup>*, and *Cd22<sup>c</sup>* encoding CD22.1, CD22.2, and CD22.3, respectively.<sup>44,45</sup> The *Cd22* gene is allelic to a lupus-susceptibility locus in New Zealand White mice, which bear *Cd22<sup>a</sup>* alleles.<sup>46</sup> *Cd22<sup>a</sup>* B cells constitutively express significantly lower levels of CD22, and do not up-regulate them on activation, to the same levels as *Cd22<sup>b</sup>* B cells.<sup>47</sup> Recently identified *Cd22<sup>c</sup>* is specifically expressed in the autoimmune-prone BXSB mouse.<sup>45</sup> Remarkably, these three alleles have striking differences in the most distal extracellular regions con-



stituting the ligand-binding domains. However, no mutation was found in CD22 sequence from TSK/+ mice (data not shown). Therefore, it is possible that factors affecting *cis*- and *trans*-binding levels of CD22 with its ligands may result in CD22 dysregulation and thereby induce autoimmunity in TSK/+ B cells (Figure 8).

B cell roles in the pathogenesis of TSK syndrome are still controversial. Kasturi and colleagues<sup>48</sup> have reported that mature B cell loss does not abrogate dermal thickening in TSK/+ mice. By contrast, adoptive transfer of both T and B cells from TSK/+ mice induces cutaneous collagen deposition and autoAb production in wild-type mice, whereas the infusion of purified T cells does not lead to the development of TSK syndrome.<sup>49</sup> A recent study has also demonstrated that disrupting the interleukin (IL)-4/IL-4R rescues TSK phenotype.<sup>21,50</sup> IL-4 is shown to abolish CD22-mediated B cell suppression by reducing CD22 expression on B cells.<sup>51</sup> Collectively, although B cells may not induce fibrosis solely, it is likely that B cell abnormalities in TSK/+ mice significantly contribute to the development of the syndrome cooperatively with other factors. The current study suggests that functional abnormalities of BCR signal transduction, especially CD22 inhibitory pathway, could contribute to autoimmunity in TSK/+ mice. Although abnormalities of B cell signaling in human autoimmune patients have not been studied intensively yet, the factors that constitute the CD19/CD22 regulatory loop, including Lyn, CD19, and SHP-1, are all suggested to be involved in the pathogenesis of human rheumatic diseases (Figure 8).<sup>16,23,52,53</sup> Exaggerated  $[Ca^{2+}]_i$  responses to BCR engagement have been also demonstrated in B cells from active SLE patients,<sup>54</sup> suggesting that signaling in B cells is a critical factor for disease activity. Further analyses in B cell signaling components would provide a clue for a potential therapeutic target for SSc and other systemic autoimmune diseases.

## References

- LeRoy EC, Black C, Fleischmajer R, Jablonska S, Krieg T, Medsger TAJ, Rowell N, Wollheim F: Scleroderma (systemic sclerosis): classification, subsets and pathogenesis. *J Rheumatol* 1988, 15:202-205
- Varga J, Bashey RI: Regulation of connective tissue synthesis in systemic sclerosis. *Int Rev Immunol* 1995, 12:187-199
- Green MC, Sweet HO, Bunker LE: Tight-skin, a new mutation of the mouse causing excessive growth of connective tissue and skeleton. *Am J Pathol* 1976, 82:493-512
- Saito S, Kasturi K, Bona C: Genetic and immunologic features associated with scleroderma-like syndrome of TSK mice. *Curr Rheumatol Rep* 1999, 1:34-37
- Kielty CM, Raghunath M, Siracusa LD, Sherratt MJ, Peters R, Shuttleworth CA, Jimenez SA: The tight skin mouse: demonstration of mutant fibrillin-1 production and assembly into abnormal microfibrils. *J Cell Biol* 1998, 140:1159-1166
- Reimer G, Steen VD, Penning CA, Medsger TAJ, Tan EM: Correlates between autoantibodies to nucleolar antigens and clinical features in patients with systemic sclerosis (scleroderma). *Arthritis Rheum* 1988, 31:525-532
- Okano Y: Antinuclear antibody in systemic sclerosis (scleroderma). *Rheum Dis Clin North Am* 1996, 22:709-735
- Steen VD, Powell DL, Medsger TAJ: Clinical correlations and prognosis based on serum autoantibodies in patients with systemic sclerosis. *Arthritis Rheum* 1988, 31:196-203
- Bona C, Rothfield N: Autoantibodies in scleroderma and tightskin mice. *Curr Opin Immunol* 1994, 6:931-937
- Saito E, Fujimoto M, Hasegawa M, Komura K, Hamaguchi Y, Kaburagi Y, Nagaoka T, Takehara K, Tedder TF, Sato S: CD19-dependent B lymphocyte signaling thresholds influence skin fibrosis and autoimmunity in the tight skin mice. *J Clin Invest* 2002, 109:1453-1462
- Chan OT, Hannum LG, Haberman AM, Madaio MP, Shlomchik MJ: A novel mouse with B cells but lacking serum antibody reveals an antibody-independent role for B cells in murine lupus. *J Exp Med* 1999, 189:1639-1648
- Korganow AS, Ji H, Mangialaio S, Duchatelle V, Pelanda R, Martin T, Degott C, Kikutani H, Rajewsky K, Pasquali JL, Benoist C, Mathis D: From systemic T cell self-reactivity to organ-specific autoimmune disease via immunoglobulins. *Immunity* 1999, 10:451-461
- Edwards JC, Cambridge G: Sustained improvement in rheumatoid arthritis following a protocol designed to deplete B lymphocytes. *Rheumatology (Oxford)* 2001, 40:205-211
- Leandro MJ, Edwards JC, Cambridge G, Ehrenstein MR, Isenberg DA: An open study of B lymphocyte depletion in systemic lupus erythematosus. *Arthritis Rheum* 2002, 2002:2673-2677
- De Vita S, Zaja F, Sacco S, De Candia A, Fanin R, Ferraccioli G: Efficacy of selective B cell blockade in the treatment of rheumatoid arthritis: evidence for a pathogenetic role of B cells. *Arthritis Rheum* 2002, 46:2029-2033
- Hasler P, Zouali M: B cell receptor signaling and autoimmunity. *FASEB J* 2001, 15:2085-2098
- Carter RH, Fearon DT: CD19: lowering the threshold for antigen receptor stimulation of B lymphocytes. *Science* 1992, 256:105-107
- Goodnow CC: Pathways for self-tolerance and the treatment of autoimmune diseases. *Lancet* 2001, 357:2115-2121
- Zhou LJ, Smith HM, Waldschmidt TJ, Schwarting R, Daley J, Tedder TF: Tissue-specific expression of the human CD19 gene in transgenic mice inhibits antigen-independent B-lymphocyte development. *Mol Cell Biol* 1994, 14:3884-3894
- Sato S, Miller AS, Inaoki M, Bock CB, Jansen PJ, Tang ML, Tedder TF: CD22 is both a positive and negative regulator of B lymphocyte antigen receptor signal transduction: altered signaling in CD22-deficient mice. *Immunity* 1996, 5:551-562
- McGaha T, Saito S, Phelps RG, Gordon R, Noben-Trauth N, Paul WE, Bona C: Lack of skin fibrosis in tight skin (TSK) mice with targeted mutation in the interleukin-4R alpha and transforming growth factor-beta genes. *J Invest Dermatol* 2001, 116:136-143
- Fujimoto M, Bradney AP, Poe JC, Steeber DA, Tedder TF: Modulation of B lymphocyte antigen receptor signal transduction by a CD19/CD22 regulatory loop. *Immunity* 1999, 11:191-200
- Sato S, Hasegawa M, Fujimoto M, Tedder TF, Takehara K: Quantitative genetic variation in CD19 expression correlates with autoimmunity. *J Immunol* 2000, 165:6635-6643
- Tedder TF, Sato S, Poe JC, Fujimoto M: CD19 and CD22 regulate a B lymphocyte signal transduction pathway that contributes to autoimmunity. *Keio J Med* 2000, 49:1-13
- Sato S, Steeber DA, Jansen PJ, Tedder TF: CD19 expression levels regulate B lymphocyte development: human CD19 restores normal function in mice lacking endogenous CD19. *J Immunol* 1997, 158:4662-4669
- Fujimoto M, Poe JC, Satterthwaite AB, Wahl MI, Witte ON, Tedder TF: Complementary roles for CD19 and Bruton's tyrosine kinase in B lymphocyte signal transduction. *J Immunol* 2002, 168:5465-5476
- Kurosaki T: Genetic analysis of B cell antigen receptor signaling. *Annu Rev Immunol* 1999, 17:555-592
- O'Keefe TL, Williams GT, Davies SL, Neuberger MS: Hyperresponsive B cells in CD22-deficient mice. *Science* 1996, 274:798-801
- Otipoby KL, Andersson KB, Draves KE, Klaus SJ, Farr AG, Kerner JD, Perlmutter RM, Law CL, Clark EA: CD22 regulates thymus-independent responses and the lifespan of B cells. *Nature* 1996, 384:634-637
- Nitschke L, Carsetti R, Ocker B, Kohler G, Lamers MC: CD22 is a negative regulator of B-cell receptor signalling. *Curr Biol* 1997, 7:133-143
- Sato S, Hamaguchi Y, Hasegawa M, Takehara K: Clinical significance of anti-topoisomerase I antibody levels determined by ELISA in systemic sclerosis. *Rheumatology* 2001, 40:1135-1140
- Hu PQ, Fertig N, Medsger TAJ, Wright TM: Correlation of serum

- anti-DNA topoisomerase I antibody levels with disease severity and activity in systemic sclerosis. *Arthritis Rheum* 2003, 48:1363–1373
33. Pani G, Siminovich KA, Paige CJ: The motheaten mutation rescues B cell signaling and development in CD45-deficient mice. *J Exp Med* 1997, 18:581–588
  34. Cornall RJ, Cyster JG, Hibbs ML, Dunn AR, Otipoby KL, Clark EA, Goodnow CC: Polygenic autoimmune traits: Lyn, CD22, and SHP-1 are limiting elements of a biochemical pathway regulating BCR signaling and selection. *Immunity* 1998, 8:497–508
  35. Otipoby KL, Draves KE, Clark EA: CD22 regulates B cell receptor-mediated signals via two domains that independently recruit Grb2 and SHP-1. *J Biol Chem* 2001, 276:44315–4322
  36. Poe JC, Fujimoto M, Jansen PJ, Miller AS, Tedder TF: CD22 forms a quaternary complex with SHIP, Grb2, and Shc. A pathway for regulation of B lymphocyte antigen receptor-induced calcium flux. *J Biol Chem* 2000, 275:17420–17427
  37. Fujimoto M, Poe JC, Hasegawa M, Tedder TF: CD19 amplification of B lymphocyte Ca<sup>2+</sup> responses: a role for Lyn sequestration in extinguishing negative regulation. *J Biol Chem* 2001, 276:44820–44827
  38. Razi N, Varki A: Masking and unmasking of the sialic acid-binding lectin activity of CD22 (Siglec-2) on B lymphocytes. *Proc Natl Acad Sci USA* 1998, 95:7469–7474
  39. Jin L, McLean PA, Neel BG, Wortis HH: Sialic acid binding domains of CD22 are required for negative regulation of B cell receptor signaling. *J Exp Med* 2002, 195:1199–1205
  40. Kelm S, Gerlach J, Brossmer R, Danzer CP, Nitschke L: The ligand-binding domain of CD22 is needed for inhibition of the B cell receptor signal, as demonstrated by a novel human CD22-specific inhibitor compound. *J Exp Med* 2002, 195:1207–1213
  41. Pezzutto A, Rabinovitch PS, Dorken B, Moldenhauer G, Clark EA: Role of the CD22 human B cell antigen in B cell triggering by anti-immunoglobulin. *J Immunol* 1988, 140:1791–1795
  42. Kumanogoh A, Watanabe C, Lee I, Wang X, Shi W, Araki H, Hirata H, Iwahori K, Uchida J, Yasui T, Matsumoto M, Yoshida K, Yakura H, Pan C, Parnes JR, Kikutani H: Identification of CD72 as a lymphocyte receptor for the class IV semaphorin CD100: a novel mechanism for regulating B cell signaling. *Immunity* 2000, 13:621–631
  43. Wang X, Kumanogoh A, Watanabe C, Shi W, Yoshida K, Kikutani H: Functional soluble CD100/Sema4D released from activated lymphocytes: possible role in normal and pathologic immune responses. *Blood* 2001, 97:3498–3504
  44. Law CL, Torres RM, Sundberg HA, Parkhouse RM, Brannan CI, Copeland NG, Jenkins NA, Clark EA: Organization of the murine Cd22 locus. Mapping to chromosome 7 and characterization of two alleles. *J Immunol* 1993, 151:175–187
  45. Lajaunias F, Ibnou-Zekri N, Fossati Jimack L, Chicheportiche Y, Parkhouse RM, Mary C, Reininger L, Brighthouse G, Izui S: Polymorphisms in the Cd22 gene of inbred mouse strains. *Immunogenetics* 1999, 49:991–995
  46. Morel L, Mohan C, Yu Y, Croker BP, Tian N, Deng A, Wakeland EK: Functional dissection of systemic lupus erythematosus using congenic mouse strains. *J Immunol* 1997, 158:6019–6028
  47. Mary C, Laporte C, Parzy D, Santiago ML, Stefani F, Lajaunias F, Parkhouse RM, O'Keefe TL, Neuberger MS, Izui S, Reininger L: Dysregulated expression of the Cd22 gene as a result of a short interspersed nucleotide element insertion in Cd22a lupus-prone mice. *J Immunol* 2000, 165:2987–2996
  48. Kasturi KN, Hatakeyama A, Murai C, Gordon R, Phelps RG, Bona CA: B-cell deficiency does not abrogate development of cutaneous hyperplasia in mice inheriting the defective fibrillin-1 gene. *J Autoimmun* 1997, 10:505–517
  49. Phelps RG, Daian C, Shibata S, Fleischmajer R, Bona CA: Induction of skin fibrosis and autoantibodies by infusion of immunocompetent cells from tight skin mice into C57BL/6 Pa/Pa mice. *J Autoimmun* 1993, 6:701–718
  50. Kodera T, McGaha TL, Phelps R, Paul WE, Bona CA: Disrupting the IL-4 gene rescues mice homozygous for the tight-skin mutation from embryonic death and diminishes TGF-beta production by fibroblasts. *Proc Natl Acad Sci USA* 2002, 99:3800–3805
  51. Rudge EU, Cutler AJ, Pritchard NR, Smith KG: Interleukin 4 reduces expression of inhibitory receptors on B cells and abolishes CD22 and FcgammaRII-mediated B cell suppression. *J Exp Med* 2002, 195:1079–1085
  52. Huck S, Le Corre R, Youinou P, Zouali M: Expression of B cell receptor-associated signaling molecules in human lupus. *Autoimmunity* 2001, 33:213–224
  53. Liossis SN, Solomou EE, Dimopoulos MA, Panayiotidis P, Mavrikakis MM, Sfrikakis PP: B-cell kinase Lyn deficiency in patients with systemic lupus erythematosus. *J Invest Med* 2001, 49:157–165
  54. Liossis SN, Kovacs B, Dennis G, Kammer GM, Tsokos GC: B cells from patients with systemic lupus erythematosus display abnormal antigen receptor-mediated early signal transduction events. *J Clin Invest* 1996, 98:2549–2557